

**Temperature- and illumination-induced charge-state change in divacancies of GaTe**

A. Zubiaga\*

*Department of Applied Physics, Aalto University, Otakaari 1, 02150 Espoo, Finland*

F. Plazaola and J. A. García

*Elektrizitatea eta Elektronika & Fisika Aplikatua II Saila, Euskal Herriko Unibertsitatea, P.O. Box 644, 48080 Bilbao, Spain*

C. Martínez-Tomás and V. Muñoz-Sanjosé

*Depto de Fisica Aplicada i Elctromagnetisme, Universitat de Valencia, Dr. Moliner 50, 46100 Burjassot, Valencia, Spain*

(Received 14 January 2010; revised manuscript received 22 April 2010; published 19 May 2010)

Temperature-dependent positron annihilation lifetime spectroscopy measurements have been performed in GaTe samples, with and without illumination. The average lifetime shows a monotonous temperature evolution but the lifetime decomposition shows a rich behavior. It is produced by two types of vacancy defects. The vacancy-type defects characterized by their shorter lifetime change their charge state below 100 K and when illuminating with light of an energy of 0.8 eV.

DOI: [10.1103/PhysRevB.81.195211](https://doi.org/10.1103/PhysRevB.81.195211)

PACS number(s): 71.55.Ht, 78.70.Bj, 78.55.Hx

**I. INTRODUCTION**

Due to their strong excitonic emission, some III-VI compound semiconductors (GaS, GaSe, and GaTe) are of interest as photon detectors, solid-state lasers, and optoelectronic devices. They form layered structures where bonds within the layers are mainly covalent and the layers are bound by van der Waals forces. GaTe is the least studied among these compounds. While other III-VI semiconductors crystallize in a four-sheet intralayer stacking pattern and all the Ga-Ga bonds are perpendicular to the layer plane, GaTe has only two thirds of the Ga-Ga bonds perpendicular to the layer planes while the others lie in the layer plane.<sup>1</sup> These bonds form chains of twofold rotational symmetry inside the layers axis.<sup>2</sup> The anisotropy of the structural and electronic transport properties of bulk GaTe,<sup>3,4</sup> the refractive index,<sup>5</sup> and the physical properties under pressure<sup>6</sup> have been studied in previous works. Optical absorption experiments performed by Camassel *et al.*<sup>7</sup> at liquid-helium temperature show a strong excitonic absorption. Other authors studied the recombination of free excitons<sup>8–12</sup> by photoluminescence (PL). The free to bound and donor-acceptor pair PL recombinations in the near-band edge<sup>13–16</sup> and time resolved PL at 4 K (Ref. 17) have been also studied.

Positron-annihilation spectroscopy can unambiguously determine the vacancy nature of a defect. It has successfully been applied to investigate the structure of intrinsic defects in different compound semiconductors but it has been scarcely applied to III-VI layered semiconductors. Measurements performed on GaSe appeared to be consistent with a temperature dependence of the annihilation parameters governed by the lattice expansion, without trapping at vacancy-type defects.<sup>18</sup> The temperature dependence of the positron lifetime in GaS is also consistent with the absence of positron trapping in as-grown samples, however, in GaTe the absence of positron trapping cannot be convincingly maintained.<sup>18</sup> In order to determine the possible existence and nature of vacancy-type point defects in layered GaTe we have performed positron-annihilation experiments in the temperature range 20–300 K. The lifetime of positron at bulk

GaTe and trapped at monovacancy and divacancy have been calculated and used to help identifying the nature of the measured defects.

**II. EXPERIMENTAL**

Ingots of GaTe were grown by the Bridgman-Stockbarger method from a polycrystalline material previously synthesized using high-purity (5N) elemental gallium and tellurium. Ingots 1–2 cm in length were obtained and from these materials, the single crystals used in our study were cleaved parallel to the plane of the layers. The measured conductivities showed that all crystals were *p* type and their carrier density was on the order of  $10^{17}$ – $10^{18}$  carriers/cm<sup>3</sup>.

The source for lifetime measurements was a <sup>22</sup>NaCl solution deposited in an Al foil. The positron source was sandwiched between two identical GaTe samples. Measurements were performed using a fast coincidence system with a time resolution of 240 ps (full width at half maximum). The samples were mounted in a closed cycle He cryostat under vacuum and in complete darkness. The cryostat had an optical window for the illumination of the sample. The temperature was varied between 15 and 300 K and the samples were illuminated using a lamp attached to a monochromator. The light beam was split in three parts using optical fibers. Two of the fibers were directed to both samples in the sandwich and the third was used to measure the light flux. The energy of the light was fixed to 0.8 eV with a flux of  $10^{16}$  cm<sup>-2</sup> s<sup>-1</sup>. Light of energy lower than the band gap induces transitions involving, mainly, defect levels within the band gap (~1.78 eV at 10 K) where carriers from the valence band can be excited and get trapped at localized defects. The charge state of the defect becomes more negative and positrons may get trapped within it. This technique is useful to study donor type or midgap defects, which are typically neutral or positively charged in *p*-type materials, with the positron-annihilation spectroscopy.

**Trapping model**

The lifetime spectra were analyzed using two lifetime components,  $n(t) = I_1 / \tau_1 \times e^{-t/\tau_1} + I_2 / \tau_2 \times e^{-t/\tau_2}$ , after subtract-

ing the annihilation in the positron source (215 ps 7%, 400 ps 4%, and 1500 ps 0.5%). The corrections and the time resolution of the spectrometer were determined using a reference sample. Assuming that besides in the bulk, positrons annihilate also in one vacancy-type defect, it is possible to calculate the positron bulk lifetime of GaTe using the one vacancy model,<sup>19</sup>

$$\tau_b = \frac{\tau_1 \tau_2}{\tau_1 + \tau_2 - \bar{\tau}}. \quad (1)$$

$\tau_1$  and  $\tau_2$  are the short and long component of the positron lifetime spectra decomposition and  $\bar{\tau}$  is the average lifetime of positrons. The average lifetime is the most meaningful parameter obtained in the spectral decomposition because it can be determined with an error of 1 ps. Equation (2) calculates  $\tau_1$  within the one positron trap model,

$$\tau_1 = \tau_b \frac{\tau_2 - \bar{\tau}}{\tau_2 - \tau_b}. \quad (2)$$

The one trap model allows to predict the trapping rate and the bulk lifetime. A kinetic model similar to the one trap model has been recently used to calculate the ortho-positronium decay rate in porous silica which is correlated with the escape yield into vacuum in a similar way of the annihilation in the bulk of metals and semiconductors to the trapping rate into defects.<sup>20</sup> Calculated  $\tau_1$  is exact only when one defect traps positrons but for two or more traps the effective bulk lifetime can be used to get valuable information, too.

The trapping rate of positrons ( $\kappa_v = \mu_v[V]$ ) is a defect specific property that is characterized by its trapping coefficient ( $\mu_v$ ) and concentration ( $[V]$ ). The trapping coefficient increases at low temperatures in negative defects ( $\mu_v \propto 1/\sqrt{T}$ ) because the long-range Coulomb tail enhances the trapping.<sup>21</sup> On the other side, it is constant for neutral defects. The trapping coefficient at room temperature is typically one order of magnitude smaller for neutral than for negative defects.

When two vacancy defects trap positrons, the average lifetime is

$$\bar{\tau} = \tau_b + \frac{\kappa_{v1}(\tau_{v1} - \tau_b) + \kappa_{v2}(\tau_{v2} - \tau_b)}{1/\tau_b + \kappa_{v1} + \kappa_{v2}}. \quad (3)$$

$\kappa_{v1}$  and  $\kappa_{v2}$  are the trapping rates of both defects with lifetimes  $\tau_{v1}$  and  $\tau_{v2}$ . In a two lifetime decomposition, the shortest lifetime is

$$\tau_1 = \frac{1 + \tau_{v1}\kappa_{v1}[1 + \kappa_{v2}/(1/\tau_b - 1/\tau_{v2} + \kappa_{v1})]}{1/\tau_b + \kappa_{v1} + \kappa_{v2}}. \quad (4)$$

The expression is valid when the shortest defect lifetime component ( $\tau_{v1}$ ) is mixed with the bulk component within the shortest lifetime ( $\tau_1$ ). Equations (3) and (4) can be used to fit  $\bar{\tau}$  and  $\tau_1$ , respectively, and estimate the concentration of the measured defects. The temperature dependence of the trapping rates has to be taken into account for negative de-

fects. The trapping coefficient for semiconductors at room temperature is typically  $10^{15} \text{ s}^{-1}$  for negative defects and  $10^{14} \text{ s}^{-1}$  for neutral defects.<sup>22</sup>

### III. COMPUTATIONAL METHODS

The positron lifetimes in perfect and defected lattices of GaTe were calculated using the atomic superposition method<sup>23</sup> where the electron density and Coulomb potential are approximated by the superposition of the unperturbed atomic densities. This approximation gives lifetime values in good agreement with experimental ones because the positron-annihilation rate is an integral quantity product of the overlap of the positron and electron densities. In addition, in self-consistent calculation of electron and positron densities the positron density relaxes following the electron distribution, keeping the value of the positron-electron overlap integral approximately constant. The positron lifetime, subsequently, is not largely affected while the open volume sensed by the positron does not change. The relaxation of the atoms surrounding the defect may have larger effect on the positron lifetime. Nevertheless, it has not been taken into account due to the lack of relaxation data. The potential felt by a positron,  $V_+(\mathbf{r})$ , is constructed according to

$$V_+(\mathbf{r}) = V_C(\mathbf{r}) + V_{corr}[n_-(\mathbf{r})], \quad (5)$$

where  $V_C$  is the Coulomb potential formed by all the charges in the system,  $n_-(\mathbf{r})$  is the electron density, and  $V_{corr}$  the positron-electron correlation energy which depends on the electron density. The Schrödinger equation is solved iteratively by using a numerical relaxation method to obtain the positron wave function and its energy eigenvalue. The calculations are performed in the supercell method where the wave function is assumed to be periodic in the cell boundaries. The positron-annihilation rate, inverse of the positron lifetime, is obtained from the overlap of positron and electron densities as

$$\lambda = \pi r_0^2 c \int dr n_+(\mathbf{r}) n_-(\mathbf{r}) \gamma(\mathbf{r}) \quad (6)$$

where  $r_0$  is the classical electron radius,  $c$  is the speed of light in the vacuum,  $n_+(\mathbf{r})$  is the positron density and  $\gamma(\mathbf{r})$  is the so-called enhancement factor.  $V_{corr}[n_-(\mathbf{r})]$  and  $\gamma(\mathbf{r})$  have been calculated using the Boronski-Nieminen (BN) approximation (Ref. 24) and generalized gradient approximation (GGA) (Refs. 25 and 26).

The crystalline structure of GaTe is monoclinical with  $C_{2/m}$  space symmetry (see Fig. 1). Each primitive cell contains six molecules and the unit cell contains 12 molecules and 108 valence electrons.<sup>22,27</sup> The primitive cell of the GaTe crystalline structure has been used as the supercell for bulk calculations. The supercell for vacancy calculations is composed by 54 primitive cells (648 atoms), big enough for the density to drop to zero in the boundaries of the supercell. All the vacancies have been assumed to be in the neutral state. The Ga vacancy, the natural acceptor in GaTe, might be negative. On the other side, the Te vacancy is expected to be neutral or positively charged. The lifetime in a negatively

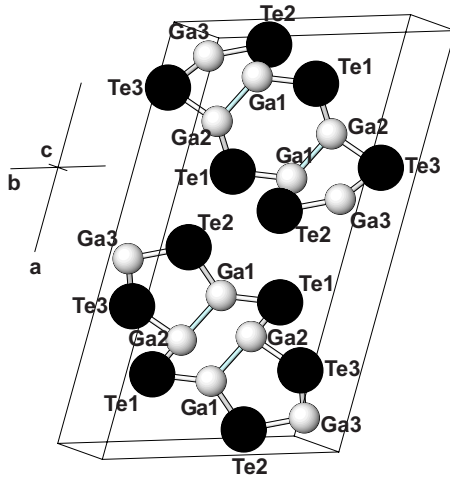


FIG. 1. (Color online) Structure of GaTe. The nonequivalent atoms are also marked.

charged defect can be shortened but this effect is normally small.<sup>28</sup>

#### IV. RESULTS AND DISCUSSION

Spectra have been decomposed into two components between 15 and 300 K with and without illumination (see Fig. 2). The average lifetime of the illuminated sample is about 4–5 ps longer for the illuminated sample than for the nonilluminated one and it increases about 3 ps from 300 to 15 K in both samples. The error bars of the decomposed values are large, particularly at low temperatures; however, the average value of  $\tau_2$  above 200 K is  $\sim 360$  ps for both samples. At lower temperatures in the illuminated sample,  $I_2$  decreases and below 130 K is very small.  $I_2$  and  $\tau_2$  have not been shown for very low temperature as their decomposition errors are large. This is an effect of the inability to resolve all the lifetime components but the average lifetime is still properly described. To overcome the large scattering of the decomposed lifetimes and intensities, the spectra have been fitted fixing  $\tau_2$  to 360 ps.

The results of the new fit are shown in Fig. 3. The average lifetime of the new fit is again 4–5 ps higher for the illuminated sample in the whole temperature range. It increases at low temperatures in the measurements performed under illumination and in darkness.  $I_2$  of the illuminated sample is about 40% from 300 to 100 K. Below 100 K, it first decreases to 20% at 70 K and increases again to 35% at 17 K. In the nonilluminated sample  $I_2$  is higher ( $\sim 50\%$ ). The short lifetime ( $\tau_1$ ) is nearly constant for both measurements above 100 K. The values of the illuminated sample are about 30 ps longer in this temperature range. Below 100 K  $\tau_1$  increases  $\sim 10$  ps (nonilluminated sample) and  $\sim 15$  ps (illuminated sample). Finally, in the illuminated sample  $\tau_1$  decreases again around 20 ps below 60 K.

It is interesting to observe that  $\bar{\tau}$  shows the same temperature behavior in both measurements. The longer average lifetime in the illumination experiment is caused by the longer  $\tau_1$  component which increases below 100 K, particularly on the illuminated sample. Such a sudden increase in  $\tau_1$  is an

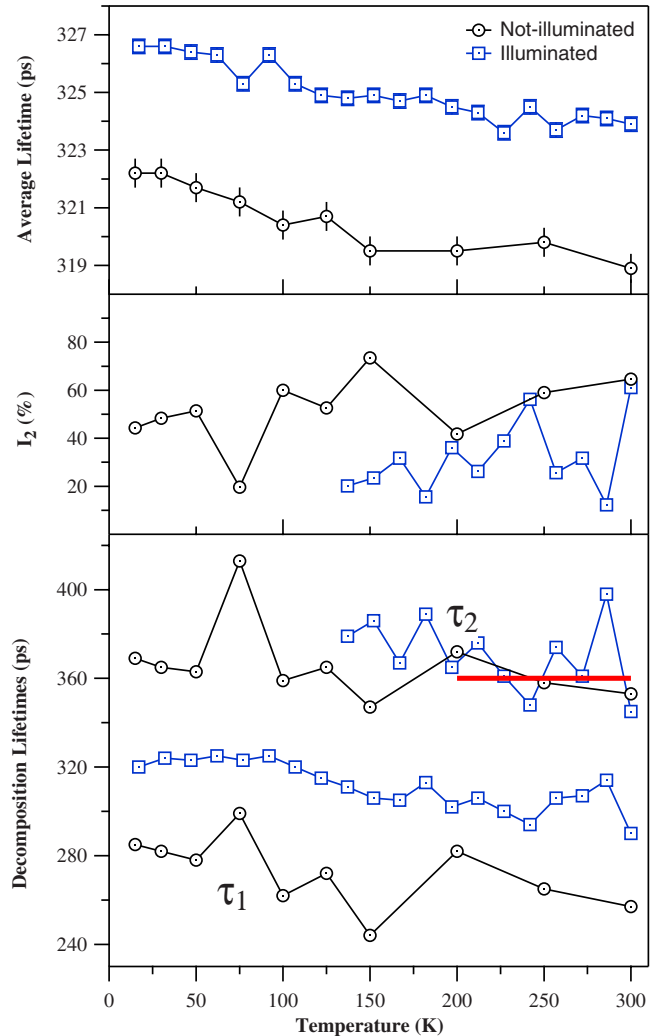


FIG. 2. (Color online) Positron average lifetime, intensity of the two lifetime components, and positron lifetimes versus the sample temperature measured with (squares) and without (circles) illumination. The full line shows the value for the second lifetime component that has been used in the subsequent analysis.

indication of a vacancy defect changing its charge state from neutral, at high temperature, to negative, below 100 K. The average lifetime does not show a large change, indicating that the lifetime of this vacancy is close to the average lifetime.

#### A. Theoretical calculations

GaTe crystal structure has three nonequivalent Ga and Te atoms giving place to three types of Ga and Te monovacancies and a high variety of divacancies (see Fig. 1). Positron lifetimes for native monovacancy and divacancy of GaTe have been calculated using BN approximation and GGA for the exchange-correlation potentials. The positron lifetime bulk value calculated using the GGA is 298 ps, around 20 ps larger than the one obtained using the BN approximation (280 ps) (see Table I). In general, GGA gives better agreement with experiment in open structures like GaTe (Refs. 23 and 26). The bulk lifetime calculated by means of GGA ex-

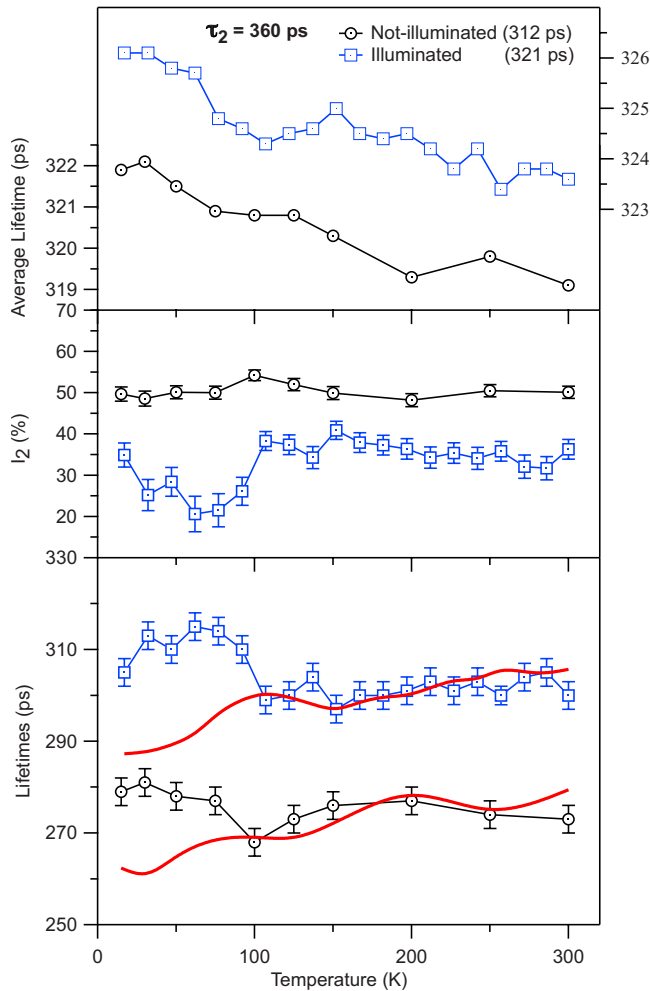


FIG. 3. (Color online) Positron average lifetime, intensity of the long lifetime component, and short positron lifetime versus the sample temperature measured with (squares) and without (circles) illumination. The long lifetime component has been fixed to be 360 ps. The full line gives the best fittings of the short lifetime using the one defect trapping model with the bulk lifetime shown in parenthesis in the legend.

plains better the high values obtained from the experimental data. Therefore, in Table I only the calculations of vacancy lifetimes performed under GGA are presented. It is worth noticing that the lifetime value calculated under BN approximation are typically 20–50 ps shorter.

The positron lifetimes in the three nonequivalent Ga monovacancies have values of 300–310 ps and they are around 50 ps shorter than the lifetimes calculated for Te monovacancies. The ratios  $\tau_d/\tau_b$  of the calculated lifetimes are always lower than the ones for monovacancies in metals.<sup>29</sup> Figure 4 shows the density distribution of the delocalized positron in bulk GaTe and in Ga<sub>3</sub>-Te<sub>3</sub> divacancy, where the positron density is well localized within the defect.

The lifetime of intrinsic monovacancy and divacancy range from 300 to 400 ps and the  $\tau_d/\tau_b$  ratio is smaller than 1.35 in all cases. The resolution of individual defect lifetimes in positron annihilation lifetime spectra can, then, be difficult and the measured lifetimes may correspond to effective values that better fit the whole lifetime distribution. The posi-

TABLE I. Lifetimes of positrons at monovacancies and first neighbor divacancies in GaTe. Atoms are labeled using the same labels of Fig. 1. Calculations are performed using the conventional scheme with BN approximation and GGA for the bulk and GGA only for the vacancies. In parenthesis, the lifetime ratio between the trapped state and the bulk is shown.

	Lifetime (ps)
Bulk (BN/GGA)	280/298
Ga	300,302,309 (1.01–1.04)
Te	359,361,364 (1.20–1.22)
Ga1-Ga2	322 (1.08)
Ga3-Ga3	363 (1.22)
(Ga1,Ga3)-Te	392,398,400 (1.32–1.34)
Ga2-Te	359,362 (1.20–1.22)

tron binding energy in Ga monovacancies, the natural acceptors of GaTe, is small, so its wave function is widespread around the defect and its lifetime is close to the bulk one. Therefore, trapping of positrons to them at room temperature will be hard to observe. The trapping and annihilation will be enhanced at very low temperatures at negatively charged Ga vacancies. On the other side, the Te vacancy is not expected to be an acceptor in GaTe and it will only trap positrons in the neutral state.

## B. Defect model

The short lifetime  $\tau_1$  has been fitted using Eq. (2) with an effective value of the bulk lifetime ( $\tau_b$ ) that fits the data above 200 K [Eq. (1)]. The effective bulk lifetimes are 312 ps for the nonilluminated sample and 321 ps for the illuminated sample. The difference in the effective bulk lifetime is a clear indication that positrons annihilating from vacancy defects also contribute to  $\tau_1$ . These unresolved defects must have a positron lifetime not far from the bulk one and from

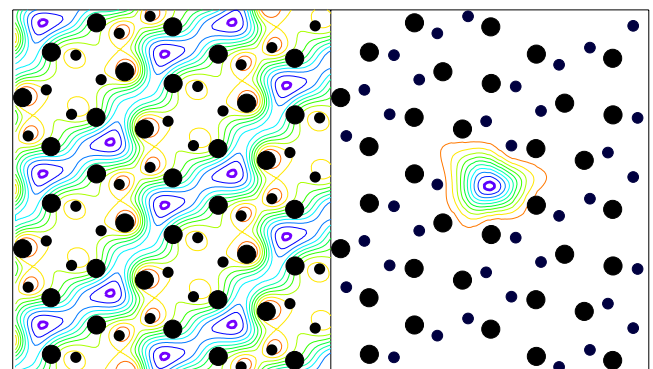


FIG. 4. (Color online) Positron density distribution in GaTe for the bulk (left panel) and the Ga<sub>3</sub>-Te<sub>3</sub> divacancy along the (001) direction. The thick (blue) contour corresponds to the maximum value of the density, subsequent contours decrease as one tenth of the maximum. Position of Ga and Te atoms are marked with small and big dots, respectively.

now on we will call them small vacancy defects. The contribution of these nonresolved small vacancies is larger in the sample measured under illumination, as indicated by their longer effective bulk lifetime. The calculated value of the effective bulk lifetime (312 ps), then, is an upper bound to the real bulk lifetime. The increased trapping at the unresolved vacancies is due to an optically induced change in the charge state from positive to neutral of small vacancy defects.

On the other side, the temperature evolution of the calculated  $\tau_1$  [Eq. (2) and Fig. 3] is similar in both samples. It remains approximately constant down to 100 K and decreases slightly at very low temperatures. At temperatures below 100 K, the calculated  $\tau_1$  does not agree with the experimental value. The lack of agreement is caused by an increase in the experimental  $\tau_1$ , correlated with the decrease in  $I_2$  indicating that the effective  $\tau_b$  is an underestimation of the actual one below 100 K. This is caused by a small vacancy defect that changes its charge state and becomes negatively charged below 100 K. The positron lifetime in them is similar to the previously commented small vacancies. The effect of the new negative vacancy is apparent in both samples but it is more pronounced in the illuminated sample. Their effect is noticeable thanks to the increased trapping coefficient in negatively charged defects compared to neutral ones (typically one order of magnitude larger). The lifetime of the small vacancies must be close to the average lifetime because then changes in their trapping will not affect appreciably the average lifetime, as we observe in our measurements (see Fig. 3).

In the illuminated sample, even though  $I_2$  increases and  $\tau_1$  decreases the average lifetime is nearly constant below 70 K (see Fig. 3). It indicates that Rydberg states with a binding energy of about 20–30 meV are created at negatively charged shallow traps at very low temperatures.<sup>30</sup> Positrons at Rydberg states annihilate with lifetimes equal to the bulk and the increased trapping at negative vacancies is compensated by the trapping in the shallow traps at very low temperatures. As result the average lifetime stays constant or decreases slightly. On the other side,  $I_2$  increases as the fraction of positrons trapped at Rydberg states increases because the nonresolved small vacancies contribute more to the long lifetime when the short lifetime decreases.

### C. Defect identification

Following Table I, the lifetime of Te monovacancies is around 360 ps, in good agreement with the long lifetime  $\tau_2$ , but they are not supposed to be natural acceptors in GaTe. Therefore, the large vacancy-type defects have been assigned to Ga-Te or Ga3-Ga3 divacancies, whose lifetimes range between 360 and 400 ps (see Table I). Their concentration, estimated using Eqs. (3) and (4), is about  $10^{17}$  cm<sup>-3</sup> in both

samples. About 5% of the vacancies are negative in the illuminated sample while it is only ~1% in the nonilluminated sample. The fraction of negative charged defects cause the smooth decrease in the average lifetime at temperatures above 200 K.

On the other side, the positron lifetime is very short in Ga monovacancies so they cannot be responsible for the small vacancy defects. A good candidate for the so-called small vacancies are Ga-Ga divacancies in Ga1 and Ga2 atom positions, whose lifetime is around 320 ps (see Table I). Their concentration has been estimated to be around  $10^{17}$  cm<sup>-3</sup> in the nonilluminated sample, one order of magnitude larger ( $10^{18}$  cm<sup>-3</sup>) in the illuminated sample. This is the reason that the effective bulk lifetime and the average lifetime are higher in the illuminated sample. Below 100 K, ~5% of the neutral small vacancies become negatively charged in both samples. Interstitials and Ga vacancies have low binding energy and can trap positrons at very low temperatures if they are negatively charged. Their lifetime is close to the bulk for positrons and their concentration is comparable to the concentration of negative defects,  $10^{16}$  cm<sup>-3</sup> in both samples.

### V. CONCLUSIONS

GaTe bulk samples have been studied using positron annihilation lifetime spectroscopy from 15 to 300 K with and without illumination. The average lifetime shows a shallow increase (4–5 ps) from room temperature to 17 K but the lifetime decomposition shows a rich behavior. Two types of vacancy defects with a concentration around  $10^{17}$  cm<sup>-3</sup> have been identified. The concentration of the small vacancy defects increases around one order of magnitude (~ $10^{18}$  cm<sup>-3</sup>) after illuminating the sample with light of an energy of 0.8 eV and ~5% become negative below 100 K. The small vacancy-type defects (positron lifetime 320 ps) have been attributed to Ga-Ga divacancies. Their lifetime is close to the average lifetime and changes in their concentration and charge state do not induce an appreciable change in  $\bar{\tau}$ . On the other side, the big vacancy-type defects (360 ps) are stable in the whole temperature range and the illumination does not affect their charge state. The concentration of negative defects is higher in the illuminated sample (up to 5% of the large vacancies). Ga-Te divacancies have been proposed as candidates for this defect. Finally, below 70 K, positrons also annihilate in shallow traps which have been attributed to Ga vacancies or to nonopen volume defects (interstitials or antisite).

### ACKNOWLEDGMENTS

We want to acknowledge the financial support from the Basque Government under Project No. IT-382-07 and the Researchers Formation Program and the Spanish MICINN under Project No. MAT2007-66129.

\*asier.zubiaga@tkk.fi

- <sup>1</sup>M. Schlüter, J. Camassel, S. Kohn, J. P. Voitchovsky, Y. R. Shen, and M. L. Cohen, *Phys. Rev. B* **13**, 3534 (1976).
- <sup>2</sup>W. B. Pearson, *Acta Crystallogr.* **17**, 1 (1964).
- <sup>3</sup>V. Augelli, C. Manfredotti, R. Murri, R. Piccolo, A. Rizzo, and L. Vasanelli, *Solid State Commun.* **21**, 575 (1977).
- <sup>4</sup>L. Gousskov, *Solid State Commun.* **28**, 99 (1978).
- <sup>5</sup>J. F. Sánchez-Royo, A. Segura, and V. Muñoz, *Phys. Status Solidi A* **151**, 257 (1995).
- <sup>6</sup>J. Pellicer-Porres, A. Segura, A. San-Miguel, and V. Muñoz, *Phys. Status Solidi B* **211**, 389 (1999).
- <sup>7</sup>J. Camassel, P. Merle, and H. Mathieu, *Physica B & C* **99**, 309 (1980).
- <sup>8</sup>J. Z. Wan, J. L. Brebner, R. Leonelli, and J. T. Graham, *Phys. Rev. B* **46**, 1468 (1992).
- <sup>9</sup>J. Z. Wan, J. L. Brebner, and R. Leonelli, *Phys. Rev. B* **52**, 16561 (1995).
- <sup>10</sup>J. Z. Wan, F. H. Pollack, J. L. Brebner, and R. Leonelli, *Solid State Commun.* **102**, 17 (1997).
- <sup>11</sup>A. Yamamoto, A. Syouji, T. Goto, E. Kulatov, K. Ohno, Y. Kawazoe, K. Uchida, and N. Miura, *Phys. Rev. B* **64**, 035210 (2001).
- <sup>12</sup>A. Syouji, A. Yamamoto, T. Goto, K. Uchida, and N. Miura, *Phys. Rev. B* **60**, 15519 (1999).
- <sup>13</sup>S. Shigetomi, T. Ikari, and H. Nishimura, *J. Lumin.* **78**, 117 (1998).
- <sup>14</sup>H. S. Güder, B. Abay, H. Efeoğlu, and Y. K. Yoğurtçu, *J. Lumin.* **93**, 243 (2001).
- <sup>15</sup>A. Zubiaga, J. A. García, F. Plazaola, V. Muñoz-Sanjosé, and M. C. Martínez-Tomás, *J. Appl. Phys.* **92**, 7330 (2002).
- <sup>16</sup>A. Zubiaga, J. A. García, F. Plazaola, V. Muñoz-Sanjosé, and C. Martínez-Tomás, *Phys. Rev. B* **68**, 245202 (2003).
- <sup>17</sup>R. A. Taylor and J. F. Ryan, *J. Phys. C* **20**, 6175 (1987).
- <sup>18</sup>R. M. de la Cruz, R. Pareja, A. Segura, V. Muñoz, and A. Chevy, *J. Phys.: Condens. Matter* **5**, 971 (1993).
- <sup>19</sup>A. Vehanen, P. Hautojärvi, J. Johansson, J. Yli-Kaupilla, and P. Moser, *Phys. Rev. B* **25**, 762 (1982).
- <sup>20</sup>L. Liskay, C. Corbel, L. Raboin, J.-P. Boilot, P. Perez, A. Brunet-Bruneau, P. Crivelli, U. Gendotti, A. Rubbia, T. Ohdaira, and R. Suzuki, *Appl. Phys. Lett.* **95**, 124103 (2009).
- <sup>21</sup>M. J. Puska and R. M. Nieminen, *Rev. Mod. Phys.* **66**, 841 (1994).
- <sup>22</sup>K. Saarinen, P. Hautojärvi, and C. Corbel, *Semiconductors and Semimetals* (Academic Press, New York, 1998), p. 209.
- <sup>23</sup>J. M. C. Robles, E. Ogando, and F. Plazaola, *J. Phys.: Condens. Matter* **19**, 176222 (2007).
- <sup>24</sup>E. Boroński and R. M. Nieminen, *Phys. Rev. B* **34**, 3820 (1986).
- <sup>25</sup>B. Barbiellini, M. J. Puska, T. Torsti, and R. M. Nieminen, *Phys. Rev. B* **51**, 7341 (1995).
- <sup>26</sup>B. Barbiellini, M. J. Puska, T. Korhonen, A. Harju, T. Torsti, and R. M. Nieminen, *Phys. Rev. B* **53**, 16201 (1996).
- <sup>27</sup>M. Julien-Pouzol, S. Jaulmes, M. Guittard, and F. Alapini, *Acta Crystallogr., Sect. B: Struct. Crystallogr. Cryst. Chem.* **35**, 2848 (1979).
- <sup>28</sup>I. Makkonen and M. J. Puska, *Phys. Rev. B* **76**, 054119 (2007).
- <sup>29</sup>N. de Diego, F. Plazaola, J. A. Jiménez, J. Serna, and J. del Río, *Acta Mater.* **53**, 163 (2005).
- <sup>30</sup>F. Plazaola, K. Saarinen, L. Dobrzynski, H. Reniewicz, F. Firszt, J. Szatkowski, H. Meczynska, S. Legowski, and S. Chabik, *J. Appl. Phys.* **88**, 1325 (2000).